8th IEEE International Conference on Automation Science and Engineering
August 20-24, 2012, Seoul, Korea

Partial Feedback Linearization Control of the Three Dimensional Overhead Crane*

Le Anh Tuan, Gook-Hwan Kim, and Soon-Geul Lee

***Abstract*—Based on the partial feedback linearization, a novel nonlinear controller is analyzed and designed for three dimensional motion of overhead crane. Three control inputs composed of bridge moving, trolley travelling, and cargo hoisting forces are used to drive five state variables consisted of bridge motion, trolley movement, cargo hoisting displacement, and two cargo swing angles. The control scheme is constituted by linearly combining two components: one is got from the nonlinear feedback of actuated states and the other is received from that of un-actuated states. To verify the quality of control process, the numerical simulation is executed. The received results show that the proposed controller asymptotically stabilizes all system states.**

I. INTRODUCTION

Nowadays, cargo transportation plays an important role in many industrial fields. For transporting the cargo in the short distance or the small area, such as in automotive factories, shipyards, the overhead cranes are naturally applied. To increase the productivity, the overhead cranes today are required in high speed operation. However, the fast motion of overhead cranes usually leads to the large swings of cargo and non-precise movements of trolley and bridge. This makes the dangerous and unsafe situation during the operating process. Therefore, a modern overhead crane system is normally equipped the good control strategy to reduce the cargo swings and increase the precise of crane motions. Up to now, the control problems of overhead cranes in both theory and practice have attracted many researchers in which various control techniques have been used from classical methods [1-2] to modern techniques [3-5].

Focused on nonlinear control of crane system, several approaches have been proposed such as sliding mode control [6-8], Feedback Linearization Control (FLC) [9-10], Lyapunov design [11-14], adaptive control [15-18]. The present study pursues the control of crane system using FLC direction. Let us review the previous papers in connection with FLC in literature. Park [19] provided the nonlinear controller for 2D container crane to suppress the cargo swing, track the trolley, and lift the cargo. The FLC technique was partially applied to actuated dynamics (characterized for trolley moving and cargo hoisting) to get one component of controller. Meanwhile, the anti-swing component was got from energy-based nonlinear control design. Two papers of Chen, one for 2D overhead cranes [20] and the other for 3D crane systems [21], dealt with nonlinear control using input-state linearization technique. In paper [20], the control law was got from the nonlinear feedback of actuated states (trolley moving and cargo lifting) without interesting in un-actuated state (cargo swing angle). Therefore, this control scheme cannot suppress the cargo vibration. The control scheme in paper [21], being an enhanced version of study [20], was designed based on the Partial Feedback Linearization (PFL) of actuated states. Furthermore, the damped component for reducing the cargo swings was added to the control law. Recently, a paper of Cho [22] proposed a control scheme linearly composed of nominal PD control and corrective one in which the nominal PD control law was designed by means of feedback linearization. Also, Cho [23] extended the PFL based controller in paper [22] where the adaptive component was integrated.

Motivated by studies [19-21], and improving the paper [9] for 3D motion, we design a novel nonlinear controller in which the PFL technique is applied for both actuated dynamics (characterized for trolley and bridge and cargo lifting motions) and un-actuated one (characterized for cargo swings). Unlike the controllers of Park [19] and Chen [20, 21], the proposed control scheme linearly composes of two components: one is got from the states nonlinear feedback of actuated dynamics and another is received from the PFL of un-actuated dynamics. First, a system dynamics of overhead cranes composed of five highly nonlinear second order differential equations is created. The system involves two un-actuated states and three actuated states driven by three control inputs. Since 3D overhead crane is an under-actuated system, its system dynamics should be separated into actuated model and un-actuated one. Next, the actuated dynamics is "linearized" by using nonlinear feedback technique, and thus, un-actuated model is considered as internal dynamics. Afterward, considering actuated states as system outputs, a nonlinear controller is proposed to track the output trajectories to desired values. However, this nonlinear control scheme does not guarantee the convergence of un-actuated states. Therefore, the structure of this nonlinear controller should be modified to satisfy the stability condition of both actuated and un-actuated states based on the feedback linearization of all system states. The controller structure is now the linear combination of two components: one is received from the feedback linearization of actuated dynamics and the other is acquired from that of un-actuated model. Hopefully, designed controller asymptotically pulls all system responses to desired values.

This paper is structured as follows. In section 2, based on Lagrange equation, a highly nonlinear mathematical model is generated in the case of complicated operation of the overhead cranes. Section 3 designs the nonlinear controller consisted of decoupling the system dynamics, designing the control law based on partial feedback linearization, and analyzing the system stability. Simulation of system responses, and result

* Research supported by the MKE (The Ministry of Knowledge Economy) of Korea.

L. A. Tuan[1], G. H. Kim[2], are with the Kyung Hee University, Suwon, 449-701 Korea (e-mail: [1]vimaru1980@gmail.com, [2]meceng93@gmail.com).

S. G. Lee is with the Kyung Hee University, Suwon, 449-701 Korea (corresponding author; phone: 82-31-201-2506; fax: 82-31-202-8106; e-mail: sglee@ khu.ac.kr).

analysis are given in section 4. Finally, some conclusions and remarks are discussed in section 5.

II. System Dynamics

The crane system involving four masses is physically modeled as on Fig. 1. All of distributed masses of bridge are converted into a concentrated mass m_b placed in the bridge center. m_l denotes equivalent masses of hoist mechanism, m_t and m_c are masses of trolley and cargo, respectively. The overhead crane has five degrees of freedom corresponding to five generalized coordinates. Namely, $x(t)$ is trolley displacement, $z(t)$ indicates bridge motion along Oz axis, and cargo position is determined by three generalized coordinates (l,θ,φ). Hence, the generalized coordinates of system is characterized by a vector $\mathbf{q}=\begin{bmatrix} z & x & l & \varphi & \theta \end{bmatrix}^T$. In addition, frictions of cargo hoisting, trolley and bridge motions are linearly characterized by damping coefficients b_r, b_t, and b_b, respectively. The control signals u_b, u_t, and u_l correspondingly demonstrate the driving forces of trolley motion, bridge movement and cargo lifting translation.

The motion equations of crane system are created by using Lagrange's equation, the dynamics of the overhead crane [24] can be represented in the following matrix form

$$\mathbf{M}(\mathbf{q})\ddot{\mathbf{q}}+\mathbf{B}\dot{\mathbf{q}}+\mathbf{C}(\mathbf{q},\dot{\mathbf{q}})\dot{\mathbf{q}}+\mathbf{G}(\mathbf{q})=\mathbf{F} \tag{1}$$

where, $\mathbf{M}(\mathbf{q})=\mathbf{M}^T(\mathbf{q})$ is symmetric mass matrix. $\mathbf{B}$ denotes damping coefficient matrix. $\mathbf{C}(\mathbf{q},\dot{\mathbf{q}})$ is Coriolis and centrifugal matrix. $\mathbf{G}(\mathbf{q})$ indicates a gravity matrix. $\mathbf{F}$ denotes matrix of control forces of driving motors. These matrixes are determined as the below formulas

$$\mathbf{q}=\begin{bmatrix} z\\ x\\ l\\ \varphi\\ \theta \end{bmatrix}, \mathbf{M}(\mathbf{q})=\begin{bmatrix} m_{11} & 0 & m_{13} & m_{14} & m_{15}\\ 0 & m_{22} & m_{23} & 0 & m_{25}\\ m_{31} & m_{32} & m_{33} & 0 & 0\\ m_{41} & 0 & 0 & m_{44} & 0\\ m_{51} & m_{52} & 0 & 0 & m_{55} \end{bmatrix}, \mathbf{G}(\mathbf{q})=\begin{bmatrix} 0\\ 0\\ g_3\\ g_4\\ g_5 \end{bmatrix},$$

$$\mathbf{B}=\begin{bmatrix} b_b & 0 & 0 & 0 & 0\\ 0 & b_t & 0 & 0 & 0\\ 0 & 0 & b_r & 0 & 0\\ 0 & 0 & 0 & 0 & 0\\ 0 & 0 & 0 & 0 & 0 \end{bmatrix}, \mathbf{C}(\mathbf{q},\dot{\mathbf{q}})=\begin{bmatrix} 0 & 0 & c_{13} & c_{14} & c_{15}\\ 0 & 0 & c_{23} & 0 & c_{25}\\ 0 & 0 & 0 & c_{34} & c_{35}\\ 0 & 0 & c_{43} & c_{44} & c_{45}\\ 0 & 0 & c_{53} & c_{54} & c_{55} \end{bmatrix}, \mathbf{F}=\begin{bmatrix} u_b\\ u_t\\ u_l\\ 0\\ 0 \end{bmatrix}.$$

The coefficients of $\mathbf{M}(\mathbf{q})$ matrix are given by

$$m_{11}=m_t+m_b+m_c,\ m_{13}=m_{31}=m_c\sin\varphi\cos\theta,$$
$$m_{14}=m_{41}=m_c l\cos\varphi\cos\theta,\ m_{15}=m_{51}=-m_c l\sin\varphi\sin\theta,$$
$$m_{22}=m_t+m_c,\ m_{23}=m_c\sin\theta,\ m_{25}=m_{52}=m_c l\cos\theta,$$
$$m_{32}=m_c\sin\theta,\ m_{33}=m_l+m_c,\ m_{44}=m_c l^2\cos^2\theta,\ m_{55}=m_c l^2.$$

The coefficients of $\mathbf{C}(\mathbf{q},\dot{\mathbf{q}})$ matrix are determined by

$$c_{13}=m_c\cos\varphi\cos\theta\dot{\varphi}-m_c\sin\varphi\sin\theta\dot{\theta},$$

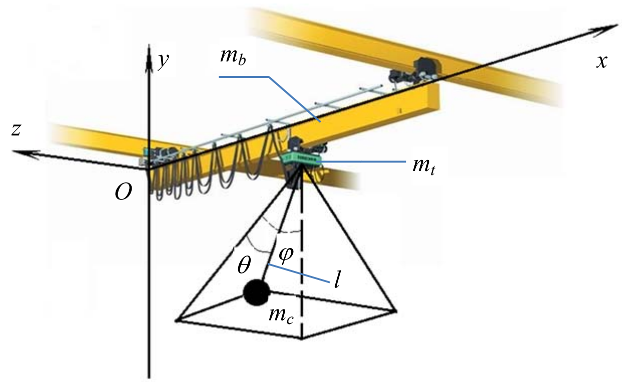

Fig. 1. Physical modeling of 3D overhead crane

$$c_{14}=m_c\cos\varphi\cos\theta\dot{l}-m_c l\cos\varphi\sin\theta\dot{\theta}-m_c l\sin\varphi\cos\theta\dot{\varphi},$$
$$c_{15}=-m_c l\cos\varphi\sin\theta\dot{\varphi}-m_c\sin\varphi\sin\theta\dot{l}-m_c l\sin\varphi\cos\theta\dot{\theta},$$
$$c_{23}=m_c\cos\theta\dot{\theta},\ c_{25}=m_c\cos\theta\dot{l}-m_c l\sin\theta\dot{\theta},$$
$$c_{34}=-m_c l\cos^2\theta\dot{\varphi},\ c_{35}=-m_c l\dot{\theta},\ c_{43}=m_c l\cos^2\theta\dot{\varphi},$$
$$c_{44}=m_c l\cos^2\theta\dot{l}-m_c l^2\cos\theta\sin\theta\dot{\theta},\ c_{45}=-m_c l^2\cos\theta\sin\theta\dot{\varphi},$$
$$c_{53}=m_c l\dot{\theta},\ c_{54}=m_c l^2\cos\theta\sin\theta\dot{\varphi},\ c_{55}=m_c l\dot{l}.$$

The nonzero coefficients of $\mathbf{G}(\mathbf{q})$ vector are given by

$$g_3=-m_c g\cos\varphi\cos\theta,\ g_4=m_c gl\sin\varphi\cos\theta,\ g_5=m_c gl\cos\varphi\sin\theta.$$

III. Control Scheme Design

A. Decoupling

Overhead crane is an under-actuated system in which five output signals are driven by three actuators. Its mathematical model should be separated into two auxiliary system dynamics: actuated and un-actuated systems. Correspondingly, $\mathbf{q}_1=\begin{bmatrix} z & x & l \end{bmatrix}^T$ for actuated states and $\mathbf{q}_2=\begin{bmatrix} \varphi & \theta \end{bmatrix}^T$ for un-actuated states are defined. Now, the matrix differential equation (1) can be detached into two equations as follows

$$\begin{pmatrix} \mathbf{M}_{11}(\mathbf{q})\ddot{\mathbf{q}}_1+\mathbf{M}_{12}(\mathbf{q})\ddot{\mathbf{q}}_2+\mathbf{B}_{11}\dot{\mathbf{q}}_1\\ +\mathbf{C}_{11}(\mathbf{q},\dot{\mathbf{q}})\dot{\mathbf{q}}_1+\mathbf{C}_{12}(\mathbf{q},\dot{\mathbf{q}})\dot{\mathbf{q}}_2+\mathbf{G}_1(\mathbf{q}) \end{pmatrix}=\mathbf{U} \tag{2}$$

$$\begin{pmatrix} \mathbf{M}_{21}(\mathbf{q})\ddot{\mathbf{q}}_1+\mathbf{M}_{22}(\mathbf{q})\ddot{\mathbf{q}}_2+\mathbf{C}_{21}(\mathbf{q},\dot{\mathbf{q}})\dot{\mathbf{q}}_1\\ +\mathbf{C}_{22}(\mathbf{q},\dot{\mathbf{q}})\dot{\mathbf{q}}_2+\mathbf{G}_2(\mathbf{q}) \end{pmatrix}=\mathbf{0} \tag{3}$$

where,

$$\mathbf{M}_{11}(\mathbf{q})=\begin{bmatrix} m_{11} & 0 & m_{13}\\ 0 & m_{22} & m_{23}\\ m_{31} & m_{32} & m_{33} \end{bmatrix}, \mathbf{M}_{12}(\mathbf{q})=\begin{bmatrix} m_{14} & m_{15}\\ 0 & m_{25}\\ 0 & 0 \end{bmatrix},$$

$$\mathbf{M}_{21}(\mathbf{q})=\begin{bmatrix} m_{41} & 0 & 0\\ m_{51} & m_{52} & 0 \end{bmatrix}, \mathbf{M}_{22}(\mathbf{q})=\begin{bmatrix} m_{44} & 0\\ 0 & m_{55} \end{bmatrix},$$

$$\mathbf{C}_{11}(\mathbf{q},\dot{\mathbf{q}})=\begin{bmatrix} 0 & 0 & c_{13}\\ 0 & 0 & c_{23}\\ 0 & 0 & 0 \end{bmatrix}, \mathbf{C}_{12}(\mathbf{q},\dot{\mathbf{q}})=\begin{bmatrix} c_{14} & c_{15}\\ 0 & c_{25}\\ c_{34} & c_{35} \end{bmatrix},$$

$$\mathbf{C}_{21}(\mathbf{q},\dot{\mathbf{q}})=\begin{bmatrix}0 & 0 & c_{43}\\ 0 & 0 & c_{53}\end{bmatrix},\ \mathbf{C}_{22}(\mathbf{q},\dot{\mathbf{q}})=\begin{bmatrix}c_{44} & c_{45}\\ c_{54} & c_{55}\end{bmatrix},$$

$$\mathbf{B}_{11}=\begin{bmatrix}b_t & 0 & 0\\ 0 & b_b & 0\\ 0 & 0 & b_r\end{bmatrix},\ \mathbf{G}_1=\begin{bmatrix}0\\ 0\\ g_3\end{bmatrix},\ \mathbf{G}_2=\begin{bmatrix}g_4\\ g_5\end{bmatrix},\ \mathbf{U}=\begin{bmatrix}u_b\\ u_t\\ u_l\end{bmatrix}.$$

The actuated equation (2) shows the direct constraint between actuated states $\mathbf{q}_1$ and actuators $\mathbf{U}$. However, un-actuated equation (3) does not display the relationship between un-actuated states $\mathbf{q}_2$ and inputs $\mathbf{U}$. Physically, the input signals $\mathbf{U}$ directly control the actuated states $\mathbf{q}_1$ and indirectly drive un-actuated states $\mathbf{q}_2$.

B. Partial Feedback Linearization

Let us transfer the dynamics of closed-loop system composed of (2) and (3) into equivalent linear form based on nonlinear feedback technique. Note that $\mathbf{M}_{22}(\mathbf{q})$ is a positive definite matrix for every $l>0$ and $|\theta|<\pi/2$, the un-actuated states $\mathbf{q}_2$ can be determined from (3) as follows

$$\ddot{\mathbf{q}}_2=-\mathbf{M}_{22}^{-1}(\mathbf{q})\begin{pmatrix}\mathbf{M}_{21}(\mathbf{q})\ddot{\mathbf{q}}_1+\mathbf{C}_{21}(\mathbf{q},\dot{\mathbf{q}})\dot{\mathbf{q}}_1\\ +\mathbf{C}_{22}(\mathbf{q},\dot{\mathbf{q}})\dot{\mathbf{q}}_2+\mathbf{G}_2(\mathbf{q})\end{pmatrix} \tag{4}$$

Observe that the cargo swings $\mathbf{q}_2=[\varphi \quad \theta]^T$ is directly concerned with properties of trolley motion x, bridge motion z and the length of wire rope l. Substituting (4) into (2) and simplifying lead to

$$\bar{\mathbf{M}}(\mathbf{q})\ddot{\mathbf{q}}_1+\bar{\mathbf{C}}_1(\mathbf{q},\dot{\mathbf{q}})\dot{\mathbf{q}}_1+\bar{\mathbf{C}}_2(\mathbf{q},\dot{\mathbf{q}})\dot{\mathbf{q}}_2+\bar{\mathbf{G}}(\mathbf{q})=\mathbf{U} \tag{5}$$

where,

$$\bar{\mathbf{M}}(\mathbf{q})=\mathbf{M}_{11}(\mathbf{q})-\mathbf{M}_{12}(\mathbf{q})\mathbf{M}_{22}^{-1}(\mathbf{q})\mathbf{M}_{21}(\mathbf{q}),$$
$$\bar{\mathbf{C}}_1(\mathbf{q},\dot{\mathbf{q}})=\mathbf{B}_{11}+\mathbf{C}_{11}(\mathbf{q},\dot{\mathbf{q}})-\mathbf{M}_{12}(\mathbf{q})\mathbf{M}_{22}^{-1}(\mathbf{q})\mathbf{C}_{21}(\mathbf{q},\dot{\mathbf{q}}),$$
$$\bar{\mathbf{C}}_2(\mathbf{q},\dot{\mathbf{q}})=\mathbf{C}_{12}(\mathbf{q},\dot{\mathbf{q}})-\mathbf{M}_{12}(\mathbf{q})\mathbf{M}_{22}^{-1}(\mathbf{q})\mathbf{C}_{22}(\mathbf{q},\dot{\mathbf{q}}),$$
$$\bar{\mathbf{G}}(\mathbf{q})=\mathbf{G}_1(\mathbf{q})-\mathbf{M}_{12}(\mathbf{q})\mathbf{M}_{22}^{-1}(\mathbf{q})\mathbf{G}_2(\mathbf{q}).$$

Note that matrices $\bar{\mathbf{M}}(\mathbf{q})$ is positive definite for every $l>0$, $|\varphi|<\pi/2$ and $|\theta|<\pi/2$. Equation (5) can be represented as

$$\ddot{\mathbf{q}}_1=\bar{\mathbf{M}}^{-1}(\mathbf{q})\left(\mathbf{U}-\bar{\mathbf{C}}_1(\mathbf{q},\dot{\mathbf{q}})\dot{\mathbf{q}}_1-\bar{\mathbf{C}}_2(\mathbf{q},\dot{\mathbf{q}})\dot{\mathbf{q}}_2-\bar{\mathbf{G}}(\mathbf{q})\right) \tag{6}$$

Substituting (6) into (4) yields

$$\ddot{\mathbf{q}}_2=-\mathbf{M}_{22}^{-1}(\mathbf{q})\begin{pmatrix}\mathbf{M}_{21}(\mathbf{q})\bar{\mathbf{M}}^{-1}(\mathbf{q})\begin{pmatrix}\mathbf{U}-\bar{\mathbf{C}}_1(\mathbf{q},\dot{\mathbf{q}})\dot{\mathbf{q}}_1\\ -\bar{\mathbf{C}}_2(\mathbf{q},\dot{\mathbf{q}})\dot{\mathbf{q}}_2-\bar{\mathbf{G}}(\mathbf{q})\end{pmatrix}\\ +\mathbf{C}_{21}(\mathbf{q},\dot{\mathbf{q}})\dot{\mathbf{q}}_1+\mathbf{C}_{22}(\mathbf{q},\dot{\mathbf{q}})\dot{\mathbf{q}}_2+\mathbf{G}_2(\mathbf{q})\end{pmatrix} \tag{7}$$

Therefore, the physical behavior of crane system can be characterized by actuated dynamics (6) and un-actuated dynamics (7) in which the mathematical relationships between $\mathbf{q}_1$, $\mathbf{q}_2$ and $\mathbf{U}$ can be seen clearly.

Considering actuated states $\mathbf{q}_1$ as the system outputs, one can "linearize" the actuated dynamics (6) by defining

$$\ddot{\mathbf{q}}_1=\mathbf{V}_a \tag{8}$$

with $\mathbf{V}_a\in\mathbf{R}^3$ being the equivalent control inputs. Then, the control signals $\mathbf{U}$ become

$$\mathbf{U}=\bar{\mathbf{M}}(\mathbf{q})\mathbf{V}_a+\bar{\mathbf{C}}_1(\mathbf{q},\dot{\mathbf{q}})\dot{\mathbf{q}}_1+\bar{\mathbf{C}}_2(\mathbf{q},\dot{\mathbf{q}})\dot{\mathbf{q}}_2+\bar{\mathbf{G}}(\mathbf{q}) \tag{9}$$

Now, let us design the controller $\mathbf{U}$ to drive the actuated states $\mathbf{q}_1=[z \quad x \quad l]^T$ reach to desired constant values $\mathbf{q}_{1d}=[z_d \quad x_d \quad l_d]^T$. In order to track the given state trajectories, the equivalent control inputs are chosen as

$$\mathbf{V}_a=\ddot{\mathbf{q}}_{1d}-\mathbf{K}_{ad}(\dot{\mathbf{q}}_1-\dot{\mathbf{q}}_{1d})-\mathbf{K}_{ap}(\mathbf{q}_1-\mathbf{q}_{1d}) \tag{10}$$

Since $\mathbf{q}_{1d}=\mathbf{const}$, the expression (10) can be reduced in the form as

$$\mathbf{V}_a=-\mathbf{K}_{ad}\dot{\mathbf{q}}_1-\mathbf{K}_{ap}(\mathbf{q}_1-\mathbf{q}_{1d}) \tag{11}$$

where, $\mathbf{K}_{ad}=\mathrm{diag}(K_{ad1},K_{ad2},K_{ad3})$, $\mathbf{K}_{ap}=\mathrm{diag}(K_{ap1},K_{ap2},K_{ap3})$ are positive diagonal matrices.

Referring to (10) and active dynamics (8), one obtains the differential equation of tracking error described by

$$\ddot{\tilde{\mathbf{q}}}_1+\mathbf{K}_{ad}\dot{\tilde{\mathbf{q}}}_1+\mathbf{K}_{ap}\tilde{\mathbf{q}}_1=\mathbf{0} \tag{12}$$

with $\tilde{\mathbf{q}}_1=\mathbf{q}_1-\mathbf{q}_{1d}$ being tracking error vector of actuated states. Clearly, dynamics of tracking error (12) is exponential stable for every $\mathbf{K}_{ad}>\mathbf{0}$ and $\mathbf{K}_{ap}>\mathbf{0}$ (with initial condition $\tilde{\mathbf{q}}_1(0)=\mathbf{0}$, $\tilde{\mathbf{q}}_1(t)\equiv\mathbf{0}\ \forall t>0$). In other words, tracking errors of actuated states $\tilde{\mathbf{q}}_1$ approaches to zeros (or $\mathbf{q}_1$ converges to $\mathbf{q}_{1d}$) as t tends to infinity. More precisely, equivalent control $\mathbf{V}_a$ forces actuated states $\mathbf{q}_1$ reach to references $\mathbf{q}_{1d}$ asymptotically.

The control scheme (9) corresponding to equivalent input $\mathbf{V}_a$ is only used for asymptotically stabilizing the actuated states $\mathbf{q}_1$. To stabilize un-actuated states $\mathbf{q}_2$, one can apply the nonlinear feedback method to sub-dynamics (7) as follows

$$\ddot{\mathbf{q}}_2=\mathbf{V}_u=-\mathbf{K}_{ud}\dot{\mathbf{q}}_2-\mathbf{K}_{up}\mathbf{q}_2 \tag{13}$$

where, $\mathbf{V}_u\in\mathbf{R}^2$ are the equivalent inputs of un-actuated states. $\mathbf{K}_{ud}=\mathrm{diag}(K_{ud1},K_{ud2})$ and $\mathbf{K}_{up}=\mathrm{diag}(K_{up1},K_{up2})$ are positive matrices. The control input $\mathbf{U}$ received from (7) and (13) assures the stability of un-actuated states $\mathbf{q}_2$ since the tracking error dynamics

$$\ddot{\mathbf{q}}_2+\mathbf{K}_{ud}\dot{\mathbf{q}}_2+\mathbf{K}_{up}\mathbf{q}_2=\mathbf{0} \tag{14}$$

is stable for every for every $\mathbf{K}_{ud}>\mathbf{0}$ and $\mathbf{K}_{up}>\mathbf{0}$. In other words, if $\mathbf{K}_{ud}$ and $\mathbf{K}_{up}$ is selected properly, the equivalent inputs $\mathbf{V}_u$ drive the cargo swings $\mathbf{q}_2=[\varphi \quad \theta]^T$ approach to zeros.

For stabilizing both un-actuated and actuated states, the overall equivalent inputs is proposed by linearly combining between $\mathbf{V}_a$ and $\mathbf{V}_u$ as follows

$$\begin{aligned}\mathbf{V} &= \mathbf{V}_a + \boldsymbol{\alpha}\mathbf{V}_u \\ &= -\mathbf{K}_{ad}\dot{\mathbf{q}}_1 - \mathbf{K}_{ap}\left(\mathbf{q}_1 - \mathbf{q}_{1d}\right) - \boldsymbol{\alpha}\left(\mathbf{K}_{ud}\dot{\mathbf{q}}_2 + \mathbf{K}_{up}\mathbf{q}_2\right)\end{aligned} \tag{15}$$

with $\boldsymbol{\alpha} = \begin{bmatrix} \alpha_1 & 0 \\ 0 & \alpha_2 \\ 0 & 0 \end{bmatrix}$ being a weighting matrix and $\mathbf{V} \in \mathbf{R}^3$.

Hence, considering $\mathbf{q}_1$ as the primary outputs, the total control scheme is determined by replacing $\mathbf{V}_a$ by $\mathbf{V}$ in the expression (9). Substituting (15) into (9), one obtains the partial feedback linearization control structure as

$$\begin{aligned}\mathbf{U} = &\left(\bar{\mathbf{C}}_1(\mathbf{q},\dot{\mathbf{q}}) - \bar{\mathbf{M}}(\mathbf{q})\mathbf{K}_{ad}\right)\dot{\mathbf{q}}_1 + \left(\bar{\mathbf{C}}_2(\mathbf{q},\dot{\mathbf{q}}) - \bar{\mathbf{M}}(\mathbf{q})\boldsymbol{\alpha}\mathbf{K}_{ud}\right)\dot{\mathbf{q}}_2 \\ &-\bar{\mathbf{M}}(\mathbf{q})\mathbf{K}_{ap}\left(\mathbf{q}_1 - \mathbf{q}_{1d}\right) - \bar{\mathbf{M}}(\mathbf{q})\boldsymbol{\alpha}\mathbf{K}_{up}\mathbf{q}_2 + \bar{\mathbf{G}}(\mathbf{q})\end{aligned} \tag{16}$$

As we will see on simulation and experiment section, the nonlinear controller (16) asymptotically stabilizes all system state trajectories.

C. Local Stability of Internal Dynamics

The control law $\mathbf{U}$ is referred from actuated dynamics (6). Let us analyze the stability of remaining part (un-actuated part) of closed-loop system called internal dynamics. If the internal dynamics is stable, our tracking control problem has been solved. Substituting control scheme (16) into un-actuated subsystem (7) yields the internal dynamics

$$\ddot{\mathbf{q}}_2 = -\mathbf{M}_{22}^{-1}(\mathbf{q})\begin{pmatrix} -\mathbf{M}_{21}(\mathbf{q})\begin{pmatrix}\mathbf{K}_{ad}\dot{\mathbf{q}}_1 + \boldsymbol{\alpha}\mathbf{K}_{ud}\dot{\mathbf{q}}_2 \\ +\mathbf{K}_{ap}\left(\mathbf{q}_1 - \mathbf{q}_{1d}\right) + \boldsymbol{\alpha}\mathbf{K}_{up}\mathbf{q}_2\end{pmatrix} \\ +\mathbf{C}_{21}(\mathbf{q},\dot{\mathbf{q}})\dot{\mathbf{q}}_1 + \mathbf{C}_{22}(\mathbf{q},\dot{\mathbf{q}})\dot{\mathbf{q}}_2 + \mathbf{G}_2(\mathbf{q})\end{pmatrix} \tag{17}$$

The local stability of internal dynamics is guaranteed if the zero-dynamics is exponentially stable. Setting $\mathbf{q}_1 = \mathbf{q}_{1d}$ in the internal dynamics (17), we obtain the zero-dynamics of system as

$$\ddot{\mathbf{q}}_2 + \mathbf{M}_{22}^{-1}(\mathbf{q})\begin{pmatrix}\left(\mathbf{C}_{22}(\mathbf{q},\dot{\mathbf{q}}) - \mathbf{M}_{21}(\mathbf{q})\boldsymbol{\alpha}\mathbf{K}_{ud}\right)\dot{\mathbf{q}}_2 \\ -\mathbf{M}_{21}(\mathbf{q})\boldsymbol{\alpha}\mathbf{K}_{up}\mathbf{q}_2 + \mathbf{G}_2(\mathbf{q})\end{pmatrix} = \mathbf{0} \tag{18}$$

which is expanded into two following expressions

$$\begin{pmatrix} l_d\ddot{\varphi} - 2l_d\tan\theta\dot{\theta}\dot{\varphi} - \alpha_1 K_{ud1}\dfrac{\cos\varphi}{\cos\theta}\dot{\varphi} \\ -\alpha_1 K_{up1}\dfrac{\cos\varphi}{\cos\theta}\varphi + g\dfrac{\sin\varphi}{\cos\theta}\end{pmatrix} = 0 \tag{19}$$

$$\begin{pmatrix} l_d\ddot{\theta} + l_d\cos\theta\sin\theta\dot{\varphi}^2 + \alpha_1 K_{ud1}\sin\varphi\sin\theta\dot{\varphi} \\ -\alpha_2 K_{ud2}\cos\theta\dot{\theta} + \alpha_1 K_{up1}\sin\varphi\sin\theta\varphi \\ -\alpha_2 K_{up2}\cos\theta\theta + g\cos\varphi\sin\theta\end{pmatrix} = 0 \tag{20}$$

The stability of zero-dynamics consisted of (19) and (20) is analyzed by using the Lyapunov's linearization theorem. First, we represent the zero-dynamics in the first-order form by setting four state variables

$$z_1 = \varphi, z_2 = \dot{\varphi},\ z_3 = \theta, z_4 = \dot{\theta}.$$

Then, the zero-dynamics is of the following state-space form

$$\dot{z}_1 = z_2 \tag{21}$$

$$\dot{z}_2 = \begin{pmatrix} 2\tan z_3 z_4 z_2 + \dfrac{\alpha_1 K_{ud1}}{l_d}\dfrac{\cos z_1}{\cos z_3}z_2 \\ +\dfrac{\alpha_1 K_{up1}}{l_d}\dfrac{\cos z_1}{\cos z_3}z_1 - \dfrac{g}{l_d}\dfrac{\sin z_1}{\cos z_3}\end{pmatrix} = f(\mathbf{z}) \tag{22}$$

$$\dot{z}_3 = z_4 \tag{23}$$

$$\dot{z}_4 = \begin{pmatrix} -\cos z_3\sin z_3 z_2^2 - \dfrac{\alpha_1 K_{ud1}}{l_d}\sin z_1\sin z_3 z_2 \\ +\dfrac{\alpha_2 K_{ud2}}{l_d}\cos z_3 z_4 - \dfrac{\alpha_1 K_{up1}}{l_d}\sin z_1\sin z_3 z_1 \\ +\dfrac{\alpha_2 K_{up2}}{l_d}\cos z_3 z_3 - \dfrac{g}{l_d}\cos z_1\sin z_3\end{pmatrix} = g(\mathbf{z}) \tag{24}$$

with $\mathbf{z} = \begin{bmatrix} z_1 & z_2 & z_3 & z_4\end{bmatrix}^T$ being a state vector. The nonlinear zero-dynamics (21)–(24) is asymptotically stable around the equilibrium point $\mathbf{z} = \mathbf{0}$ ($\mathbf{q}_2 = \dot{\mathbf{q}}_2 = \mathbf{0}$) if the corresponding linearized system is strictly stable. Linearizing the zero-dynamics around $\mathbf{z} = \mathbf{0}$ yields the linearized system of the form

$$\dot{\mathbf{z}} = \mathbf{A}\mathbf{z} \tag{25}$$

where,

$$\begin{aligned}\mathbf{A} &= \begin{bmatrix} 0 & 1 & 0 & 0 \\ \dfrac{\partial f}{\partial z_1} & \dfrac{\partial f}{\partial z_2} & \dfrac{\partial f}{\partial z_3} & \dfrac{\partial f}{\partial z_4} \\ 0 & 0 & 0 & 1 \\ \dfrac{\partial g}{\partial z_1} & \dfrac{\partial g}{\partial z_2} & \dfrac{\partial g}{\partial z_3} & \dfrac{\partial g}{\partial z_4}\end{bmatrix}_{\mathbf{z}=\mathbf{0}} \\ &= \begin{bmatrix} 0 & 1 & 0 & 0 \\ \dfrac{\alpha_1 K_{up1} - g}{l_d} & \dfrac{\alpha_1 K_{ud1}}{l_d} & 0 & 0 \\ 0 & 0 & 0 & 1 \\ 0 & 0 & -\dfrac{g}{l_d} & \dfrac{\alpha_2 K_{ud2}}{l_d}\end{bmatrix}\end{aligned} \tag{26}$$

is a Jacobian matrix.

The linearized system (25) is stable around the equilibrium point $\mathbf{z} = \mathbf{0}$ if $\mathbf{A}$ is a Hurwitz matrix. Based on Hurwitz's criterion and after some calculation, we receive the constraint condition of controller parameters as follows

$$\left(K_{ud1}\alpha_1 + K_{ud2}\alpha_2\right) < 0 \tag{27a}$$

$$l_d\left(K_{up1}\alpha_1 - 2g\right) < K_{ud1}K_{ud2}\alpha_1\alpha_2 \tag{27b}$$

$$K_{ud1}\alpha_1 g < K_{ud2}\alpha_2\left(K_{up1}\alpha_1 - g\right) \tag{27c}$$

$$K_{up1}\alpha_1 < g \tag{27d}$$

Therefore, if the relationships (27a–d) of control parameters are held, the zero dynamics is stable around equilibrium point $\mathbf{z} = \mathbf{0}$ which leads to the local stability of internal dynamics (17).

IV. Numerical Simulation and Result Analysis

Let us numerically simulate the overhead crane dynamics (1) driven by control inputs (16) in the case of the most complicated operation of crane system. Accordingly, the trolley is forced to move from its initial position to 0.4 m desired displacement, the bridge is driven from its starting point to 0.3 m desired location, and the cargo is lifted from 1 m cable length to 0.7 m of cable reference. These processes (lifting the cargo, moving the trolley, travelling the bridge) must be begun at the same initial time. The cargo suspended cable is initially perpendicular to ground. The parameters used for simulation is given on Table. 1.

TABLE I. Crane System Parameters

System dynamics	Controller
$g = 9.81$ m/s^2, $m_c = 0.85$ kg,	$\mathbf{K}_{ad} = \mathrm{diag}(1.5, 1.5, 2.5), \mathbf{K}_{ud} = \mathrm{diag}(3,3)$
$m_t = 5$ kg, $m_b = 7$ kg, $m_l = 2$ kg,	$\mathbf{K}_{ap} = \mathrm{diag}(0.85, 0.87, 2)$
$b_t = 20$ N.m/s, $b_b = 30$ N.m/s,	$\mathbf{K}_{up} = \mathrm{diag}(0.5, 0.5)$, $\alpha_1 = \alpha_2 = -1$
$b_r = 50$ N.m/s	

The achieved results are described on Figs. 2–6. Fig. 2 describes the paths of bridge motion, trolley movement, and payload lifting translation. All trajectories asymptotically converge to references. Bridge moves and stops accurately at load endpoint after 4 seconds. Trolley comes to destination after 4.1 seconds. Cargo is lifted from 1 m initial cable length to 0.7 m desired cable length after 4.2 seconds.

The responses of cargo swings are depicted on Fig. 3. The cargo swings are bounded with small angles during the cargo transfer process, $\varphi_{\max} = 2.2^0$, $\theta_{\max} = 2.9^0$. The cargo swings are entirely suppressed after the short setting times, $t_s = 4$ s for φ-response and $t_s = 4.5$ s for θ- one, within one vibration period.

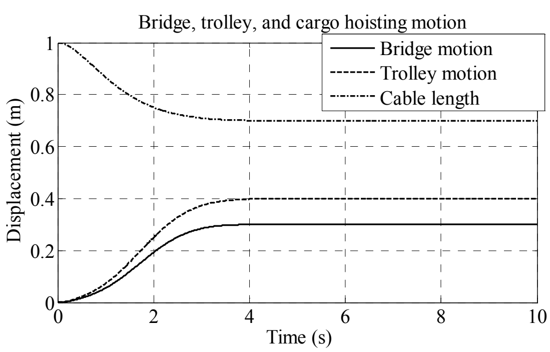

Fig. 2. Bridge, trolley, and cargo hoisting motion

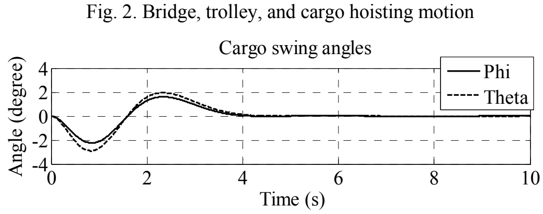

Fig. 3. Cargo swing angles (φ and θ)

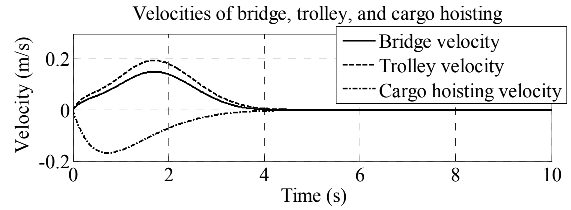

Fig. 4. Velocities of bridge, trolley, and cargo hoisting motion

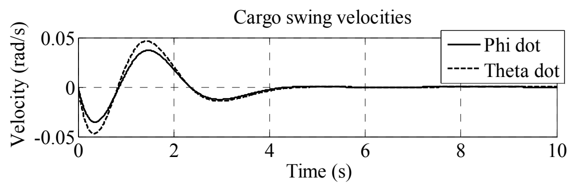

Fig. 5. Payload swing velocities ($\dot{\varphi}$ and $\dot{\theta}$)

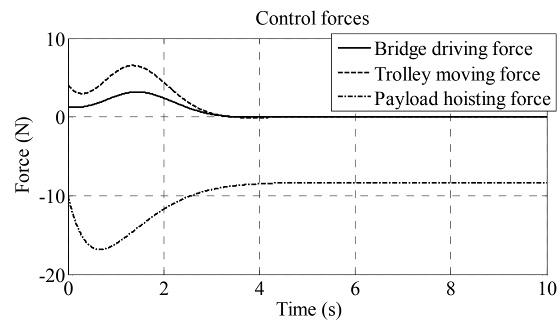

Fig. 6. Control inputs

Velocities of system responses shown on Figs. 4-5 asymptotically reach to zeros. The motions of bridge and trolley, the lifting movement of payload at transient states are composed of two stages: the increasing velocity period and the decreasing one. It is clearly that trolley speeds up within 1.7 first seconds and speed down within 2.4 remaining seconds; cargo is lifted with growing speed within 0.7 first seconds and with reducing speed within 3.5 remaining seconds.

The nonlinear control forces are illustrated on Fig. 6. The simulation responses achieve to steady states after 4 seconds for bridge moving force, 4.1 seconds for trolley moving force, and 4.2 seconds for cargo lifting one. At steady states, $u_t^{ss} = u_b^{ss} = 0$ N and $u_l^{ss} = -m_c g = -9.81 \times 0.85 = -8.34$ N.

V. Conclusion

Feedback linearization method provides an effective design tool for control of a class of under-actuated mechanical systems such as overhead crane system. Based on this technique, a nonlinear controller having good quality was designed. The simulation results show that the proposed controller stabilizes the overhead crane system. All system responses asymptotically reach to desired values within the considerable short time: bridge and trolley were controlled to move to desired position, also cargo was lifted up to the reference, precisely. Moreover, the cargo swings were kept small during transfer process, and were suppressed at load destination. In the future work, the nonlinear control design will be extended for overhead crane by combining with adaptive control technique.

ACKNOWLEDGMENT

This research was supported by the ITR C (Information Technology Research Center) support program supervised by the NIPA (National IT Indus try Promotion Agency) (NIPA-2012-C1090-1221-0013) and the program supervised by the KEIT (Korea Evaluation Institute of Industrial Technology) (No.: 10035544).

REFERENCES

[1] K. A. F. Moustafa, “Reference trajectory tracking of overhead cranes,” *Journal of Dynamics Systems, Measurement, and Control*, vol. 123, issue. 1, pp.139-141, 2001.

[2] D. Chwa, “Nonlinear tracking control of 3D overhead cranes against the initial swing angle and variation of payload weight,” *IEEE Transactions on Control Systems Technology*, vol. 17, no. 4, pp. 876-883, 2009.

[3] A. Benhidjeb and G. L. Gissinger, “Fuzzy control of an overhead crane performance comparison with classic control,” *Control Engineering Practice*, vol. 3, issue. 12, pp. 1687-1696, 1995.

[4] C. Y. Chang and K. H. Chiang, “Intelligent fuzzy accelerated method for the nonlinear 3D crane control,” *Expert System with Applications*, vol. 35, issue. 3, pp. 5750-5752, 2009.

[5] S. Garrido, M. Abderrahim, et. al., “Anti-swinging input shaping control of an automatic construction crane,” *IEEE Transactions on Automation Science and Engineering*, vol. 5, no. 3, pp. 549-557, 2008.

[6] N. Almutairi and M. Zribi, “Sliding mode control of a three dimensional overhead crane,” *Journal of Vibration and Control*, vol. 15, no. 11, pp. 1679-1730, 2009.

[7] H. H. Lee, Y. Liang, and D. Segura, “A sliding mode anti-swing trajectory control for overhead cranes with high-speed load hoisting,” *Journal of Dynamics Systems, Measurement, and Control*, vol. 128, pp.842-845, 2006.

[8] Le Anh Tuan and Soon-Geul Lee, “Sliding Mode Controls of Double-pendulum Crane Systems,” in *Proceeding of International Symposium on Dynamics and Control*, Hanoi, Vietnam, September 2011.

[9] Tuan Anh Le, Gook-Hwan Kim, Min Young Kim and Soon-Geul Lee, “Partial Feedback Linearization Control of Overhead Cranes with Varying Cable Lengths,” *International Journal of Precision Engineering and Manufacturing*, vol. 13, no. 4, pp. 501-507, April, 2012.

[10] Le Anh Tuan, Adiyabaatar Janchiv, Gook Hwan Kim, and Soon-Geul Lee, “Feedback Linearization Control of Overhead Cranes with Varying Cable Length,” in *Proceeding of International Conference on Control, Automation and Systems*, Gyeonggi-do, Korea, October, 2011.

[11] Y. Fang, W. E. Dixon, D. M. Dawson, and E. Zergeroglu, “Nonlinear coupling control laws for an under-actuated overhead crane system,” *IEEE/ASME Transactions on Mechatronics*, vol. 8, no. 3, pp. 418-423, 2003.

[12] H. C. Cho, J. W. Lee, Y. J Lee and K. S. Lee, “Lyapunov theory based robust control of complicated nonlinear mechanical systems with uncertainty,” *Journal of Mechanical Science and Technology*, vol. 22, pp. 2142-2150, 2008.

[13] H. H. Lee, “A new approach for the anti-swing control of overhead cranes with high-speed load hoisting,” *International Journal of Control*, vol. 76, no. 15, pp.1493-1499, 2003.

[14] N. Sun, Y. Fang, Y. Zhang, and B. Ma, “A novel kinematic coupling-based trajectory planning method for overhead cranes,” *IEEE/ASME Transactions on Mechatronics*, vol. 17, no. 1, pp. 166-173, Feb. 2012.

[15] G. Corriga and A. Giua, “An implicit gain-scheduling controller for cranes,” *IEEE Transactions on Control Systems Technology*, vol. 6, no. 1, pp.15-20, 1998.

[16] Y. J. Hua and Y. K. Shine, “Adaptive coupling control for overhead crane systems,” *Mechatronics*, vol. 17, issues. 2-3, pp. 143-152, 2007.

[17] J. H. Yang and S. H. Shen, “Novel approach for adaptive tracking control of a 3D overhead crane system,” *Journal of Intelligent Robot System*, vol. 62, no. 1, pp. 59-80, 2010.

[18] Le Anh Tuan, Sang-Chang Moon, Dong-Han Kim, and Soon-Geul Lee, "Adaptive Sliding Mode Control of Three Dimensional Overhead Cranes," in *Proceeding of IEEE International Conference on Cyber Technology in Automation, Control, and Intelligent Systems*, Bangkok, Thailand, May, 2012.

[19] H. Park, D. Chwa and K. S. Hong, “A feedback linearization control of Container cranes: Varying rope length,” *International Journal of Control, Automation, and Systems*, vol. 5, pp. 379-387, 2007.

[20] H. Chen, B. Gao and X. Zhang, “Nonlinear controller for a gantry crane based on a partial feedback linearization,” in *2005 International Conference on Control and Automation*, Budapest, Hungary, June 2005.

[21] H. Chen, B. Gao and X. Zhang, “Dynamical modeling and nonlinear control of a 3D overhead cranes,” in *2005 International Conference on Control and Automation*, Budapest, Hungary, June 2005.

[22] H. C. Cho and K. S. Lee, “Adaptive control and stability analysis of nonlinear crane systems with perturbation,” *Journal of Mechanical Science and Technology*, vol. 22, pp. 1091-1098, 2008.

[23] H. C. Cho, J. W. Lee, Y. J. Lee, and K. S. Lee, “Lyapunov theory based robust control of complicated nonlinear mechanical systems with uncertainty,” *Journal of Mechanical Science and Technology*, vol. 22, no. 11, pp. 2142-2150, 2008.

[24] H.-H. Lee, “Motion planning for three-dimensional overhead cranes with high-speed load hoisting,” *International Journal of Control*, vol. 78, no. 12, pp. 875-886, 2005.